Microstructured Optical Fiber Bragg Grating Sensors for Structural Health Monitoring Applications

Francis Berghmans, Thomas Geernaert, Camille Sonnenfeld, Sanne Sulejmani, Geert Luyckx, Nicolas Lammens, Joris Degrieck, Karima Chah, Hugo Thienpont

7th European Workshop on Structural Health Monitoring
July 8-11, 2014. La Cité, Nantes, France

MICROSTRUCTURED OPTICAL FIBER BRAGG GRATING SENSORS FOR STRUCTURAL HEALTH MONITORING APPLICATIONS

Francis Berghmans[1], Thomas Geernaert[1], Camille Sonnenfeld[1], Sanne Sulejmani[1], Geert Luyckx[2], Nicolas Lammens[2], Joris Degrieck[2], Karima Chah[3], Hugo Thienpont[1]

[1] *Vrije Universiteit Brussel, Department of Applied Physics and Photonics, Brussels Photonics Team, Pleinlaan 2, 1050 Brussels, Belgium*
[2] *Universiteit Gent, Department of Materials Science and Engineering, Technologiepark 903, 9052 Gent, Belgium*
[3] *Université de Mons, Department of Electromagnetism and Telecommunications, Boulevard Dolez 31, 7000 Mons, Belgium*

fberghma@vub.ac.be

ABSTRACT

We first shortly review the state-of-the-art of microstructured optical fiber Bragg grating (MOFBG) sensors for structural health monitoring applications. We then focus on a specific microstructured optical fiber (MOF) design to which we refer as 'Butterfly' MOF. This fiber is highly birefringent and encodes the transverse strain into the spectral distance between the two Bragg peaks reflected by a fiber Bragg grating fabricated in this fiber. Since the birefringence of that MOF is not sensitive to temperature changes, the transverse strain measurement is independent of temperature variations. We subsequently discuss the potential of our MOFBG sensors for structural health monitoring related applications, including three-dimensional strain measurements within composite materials, cure monitoring and residual strain quantification following composite material manufacturing, shear stress measurements in lap joints and temperature insensitive vibration monitoring.

KEYWORDS : *microstructured optical fiber, optical fiber sensor, fiber Bragg grating, structural health monitoring*

INTRODUCTION

Microstructured optical fiber Bragg grating (MOFBG) sensors are becoming increasingly popular owing to the peculiar characteristics of microstructured optical fibers (MOFs) that cannot be achieved using conventional optical fiber technology. More specifically, the design flexibility of such microstructured fibers allows developing sensors that exhibit selective sensitivities to e.g. axial strain, transverse strain or even shear stress, whilst being negligibly cross-sensitive to temperature changes. This is a great asset for structural health monitoring (SHM) applications. Section 1 of this paper will shortly summarize the state-of-the-art on the use of MOF based sensors for SHM purposes.

Section 2 focuses on a specific microstructured fiber design to which we refer as 'Butterfly' MOF. This fiber is highly birefringent and encodes the transverse strain into the spectral distance $\Delta\lambda$ between the two Bragg peaks reflected by a fiber Bragg grating (FBG) fabricated in this fiber (Figure 1). Since the birefringence of that MOF is not sensitive to temperature changes, the transverse strain measurement is independent of temperature variations. In Section 3 we show that by using this MOF, we can simultaneously measure the normal strain in 3 dimensions inside a composite - the axial strain, the transverse in-plane strain and the transverse out-of-plane strain - with μstrain resolutions using commercially available FBG interrogator equipment.

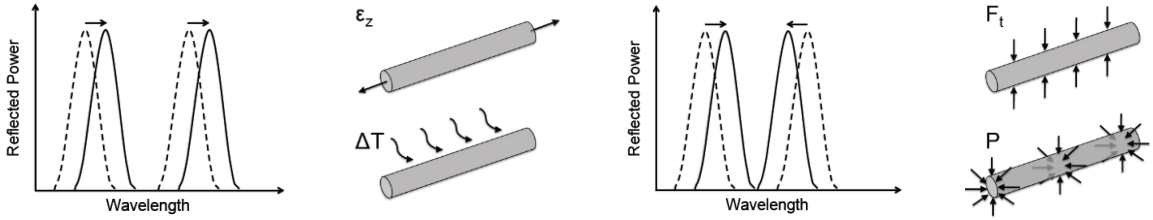

(a) (b)

Figure 1: Sensing principle of the butterfly MOFBG. Load applied transversally to the fiber is encoded in the spacing Δλ between the two Bragg peaks. (a) Response of the sensor to temperature changes or axial strain – both peaks move in the same way and Δλ remains unchanged. (b) Response of the sensor to transverse load – the peaks move in opposite direction and Δλ changes.

Finally, Section 4 deals with the potential of our MOFBG sensor for other structural health monitoring related applications, in particular cure monitoring during and residual strain quantification following composite material manufacturing, shear stress measurements in lap joints and temperature insensitive vibration monitoring.

1 STATE-OF-THE-ART OF MOF FOR SHM-RELATED APPLICATIONS

As stated above, MOF technology allows achieving optical fibers with sensing characteristics that cannot be obtained with conventional fiber technology. MOF sensing approaches and techniques have been reviewed for example by Frazao et al. [1], Canning [2] and Pinto et al. [3]. With respect to SHM related applications, MOF based sensors have been mostly combined with gratings inscribed in these fibers to enable measurements of mechanical quantities. A far from exhaustive list of examples includes pressure, transverse force, strain and bend sensing, with emphasis on avoiding strain and temperature cross-sensitivity or discriminating between strain and temperature effects [4]-[14]. Grating inscription techniques in MOF have been reviewed recently in [15].

2 THE BUTTERFLY MOF AND GRATINGS WRITTEN THEREIN

We have obtained the cross-section of our highly birefringent Butterfly MOF following extensive modeling that considered both the optical and the mechanical characteristics of the fiber [16]. We have modeled the sensitivity of the phase modal birefringence B to external thermo-mechanical perturbations with the commercially available COMSOL Multiphysics® software [17].

The phase modal birefringence B is defined as:

$$B = \frac{\lambda}{2\pi}\left(\beta_x - \beta_y\right) \tag{1}$$

where β_x and β_y are the propagation constants of the orthogonally polarized fundamental modes propagating through the MOF. When fabricating a FBG with a period Λ in a birefringent MOF, the grating will return two reflection peaks with a wavelength separation Δλ (see also Figure 1) given by:

$$\Delta\lambda = 2B\Lambda \tag{2}$$

The polarimetric pressure and temperature sensitivities K_p and K_T are defined as:

$$K_p \triangleq \frac{2\pi}{\lambda}\frac{dB}{dp}\ ;\ K_T \triangleq \frac{2\pi}{\lambda}\left(\frac{dB}{dT} + B\alpha\right) \tag{3}$$

If we want to obtain a MOF that is very sensitive to pressure whilst being – in as much as possible – insensitive to temperature changes, the figure-of-merit K_p/K_T should be maximized. To

do so one has to be able to calculate K_p and K_T. A full description of how this can be done is out of the scope of this paper. We refer to [16], [18] and [19] for a more detailed discussion.

The "Butterfly" fiber that we have obtained, with an ideal and as-built cross-section as shown in Figure 2, fulfills our requirements in terms of sensitivity, fiber manufacturability and optical guiding properties.

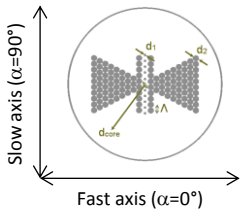

Parameter	Typical Value
Outer cladding diameter	125 µm
Number of rings of airholes	6 - 9
Airhole pitch Λ	3.5 - 4 µm
d_1/Λ	0.225
d_2/Λ	0.95 - 0.99
d_{core}/Λ	0.9
Core doping concentration	~ 2.88 mol%

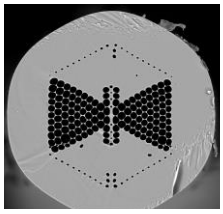

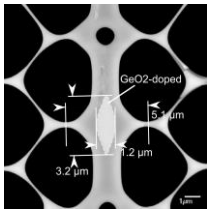

(a) (b) (c) (d)

Figure 2: (a) Ideal cross-section of the Butterfly MOF (b) Ideal parameters of the Butterfly MOF (c) Scanning Electron Microscope photograph of the cross-section of the fabricated Butterfly MOF. (d) Close-up of the core region of the MOF.

3 THREE-DIMENSIONAL STRAIN MEASUREMENTS IN COMPOSITE MATERIALS

Due to its particular structure, the sensitivity of the butterfly MOFBG to transverse strain varies in a sinusoidal manner with the angular orientation α of the microstructure with respect to the direction of the applied load. It is most sensitive when the load is applied along α = 90°, which corresponds to the direction of the slow-axis indicated in Figure 2(a) [20]. This dependence of the sensitivity on the angular orientation can be exploited to quantify the strain along the 3 directions of space inside a carbon fiber reinforced polymer (CFRP) composite material. To do so, one needs to relate the normal strains in the 3 directions of space in the composite material to the measured changes in the 4 Bragg wavelengths returned by two closely spaced MOFBG sensors embedded in a composite coupon with different angular orientations, as schematically illustrated in Figure 3.

The relation between the strains and the temperature in the material at the location of the sensors and the Bragg wavelength shifts is given by Equation (4).

$$\begin{pmatrix} \varepsilon_1^h \\ \varepsilon_2^h \\ \varepsilon_3^h \\ \Delta T \end{pmatrix} = [TC] \cdot [K]^{-1} \cdot \begin{pmatrix} \Delta\lambda_{B1,1'}/\lambda_{B1,1'} \\ \Delta\lambda_{B1,2'}/\lambda_{B1,2'} \\ \Delta\lambda_{B2,1'}/\lambda_{B2,1'} \\ \Delta\lambda_{B2,2'}/\lambda_{B2,2'} \end{pmatrix} \quad (4)$$

This equation uses the Transfer Coefficient matrix [TC] that relates the temperature and strain distributions in the host composite material to those in the optical fiber sensor in the coordinate system (1^h,2^h,3^h) of the host composite material [21],[22]. More specifically, ε_1^h is the axial strain, ε_2^h is the transverse in-plane strain and ε_3^h is the transverse out-of-plane strain (see also Figure 3). We obtained the [TC] matrix using extensive finite-element modelling. The sensitivity matrix [K] relates the temperature and strain changes in the optical fiber core to the output of the optical signal [23],[24]. This sensitivity matrix is obtained in an analytical form. $\lambda_{B1,1'}$ and $\lambda_{B1,2'}$ denote the initial unstrained Bragg wavelengths of the first MOFBG, and $\lambda_{B2,1'}$ and $\lambda_{B2,2'}$ are the initial unstrained Bragg wavelengths of the second MOFBG. $\Delta\lambda_{B1,1'}$, $\Delta\lambda_{B1,2'}$, $\Delta\lambda_{B2,1'}$ and $\Delta\lambda_{B2,2'}$ are the shifts of these Bragg wavelength peaks that stem from thermo-mechanical load applied to the composite material. The coordinates 1' and 2' associated with the two Bragg wavelengths returned by one MOFBG correspond to the directions of the slow and fast axes of the MOF, respectively (see Figure 2).

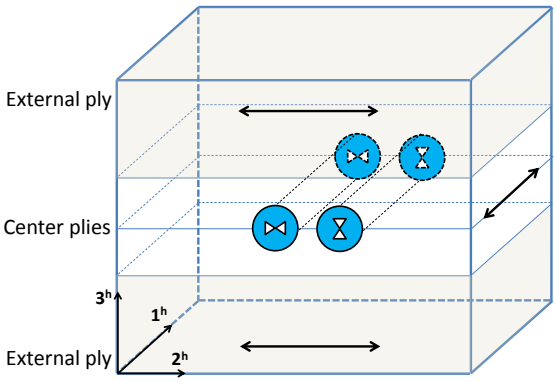

Figure 3: Illustration of 2 closely space MOFBGs embedded in the middle of a laminate composite (not drawn to scale) with the longitudinal direction of the optical fibers aligned with the reinforcement fibers of the embedding plies. The left MOFBG is oriented with α = 0°, whilst the right sensor is oriented with α = 90°. The 2 MOFBGs are stripped over a few centimeters at the grating location. The axis system (1^h,2^h,3^h) represents the coordinate system within the host composite material. The directions of the carbon reinforcement fibers in the plies are indicated by the black double arrows.

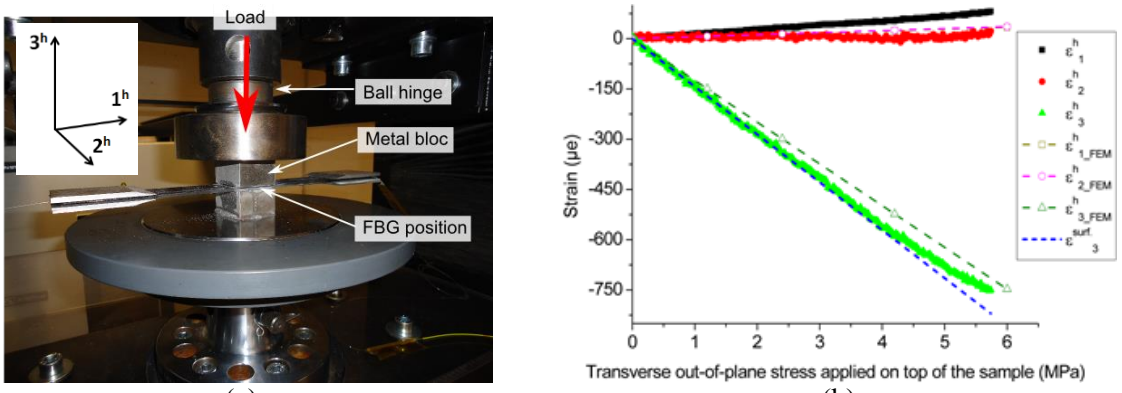

(a) (b)

Figure 4: (a) Experimental set-up used for transverse out-of-the plane loading of a CFRP coupon. The CFRP sample is compressed between two metal blocs along the direction through the thickness. The coordinate system (1^h,2^h,3^h) of the composite sample is indicated. (b) Measured strains in $[90/0]_{2s}$ and $[0/90]_{2s}$ laminates as a function of the applied transverse out-of-plane stress in isothermal conditions. ε_1^h, ε_2^h and ε_3^h have been calculated with Equation (4). $\varepsilon_{1\_FEM}^h$, $\varepsilon_{2\_FEM}^h$ and $\varepsilon_{3\_FEM}^h$ are the results of our finite element simulations. ε_3^{surf} is the strain in the direction through the thickness, calculated from the load cell reading and from the material parameters of the laminate.

Figure 4 (b) shows a typical result obtained for a transverse out-of-plane load applied to a CFRP coupon in isothermal conditions, as illustrated in Figure 4(a). We obtain a good agreement between our finite element modelling results and the strains measured and derived using Equation (4). The calculated axial strain in the composite material shows a relatively larger relative error of up to 50% when compared to the experimental data of the strain gauge. However, and since the axial strains are very low, this corresponds to a difference of only 24 με in the MOFBG configuration 0°/90° as sketched in Figure 3. The values of the transverse in-plane strain also exhibit some differences with respect to the measured strains, which can be explained by their low values. This stems from the fact that the expected strains along the 1^h- and 2^h-directions have the same magnitude as the strain measurement resolutions of about 5 με (these resolutions are not discussed in this paper). The calculated transverse out-of-the plane strains exhibit an excellent agreement with the measured strains, with a relative error around 10%.

4 OTHER SHM RELATED APPLICATIONS OF THE BUTTERFLY MOF

4.1 Composite cure monitoring and residual strain quantification

In earlier work we have shown that it is possible to efficiently integrate Butterfly MOFBG based sensors in CFRP material to monitor its manufacturing process. The sensors allow assessing the onset of polymerization and quantifying the internal residual strain in the composite material that was created as a result of the vacuum bagging autoclave process [25]-[27].

Figure 5(a) shows a scheme of the CFRP specimen in which the Butterfly MOFBG was integrated and the evolution of the Bragg wavelength separation Δλ during the cure cycle. The temperature variation recorded by thermocouple TC6 placed in close vicinity to the MOFBG is shown as well. Figure 5(b) shows a first drop of Δλ (part B) which corresponds to the polymerization of the sample. The cooling phase (part D) features a large decrease of Δλ associated with the build-up of residual strains during the consolidation phase. Since the phase modal birefringence of the Butterfly MOF is inherently insensitive to temperature, the changes in Δλ are due to thermally induced transverse strain resulting from the changing strain state in the CFRP material as it cures.

In part B Δλ decreases with 22 pm which corresponds to a compressive transverse strain of about -100 µstrain. In region C, the sensor signal remains constant meaning that no transverse strain is measured by the MOF sensor. One can therefore reasonably assume that the cure reaction has been completed and that the composite material is formed. The cooling down to room temperature (part D) is associated with a large decrease of Δλ and thus with the development of substantial transverse residual strain of about -1100 µstrain in the composite material. The conversion from change in Δλ to actual transverse strain values is obtained using data from previous sensor calibrations, as explained in [27].

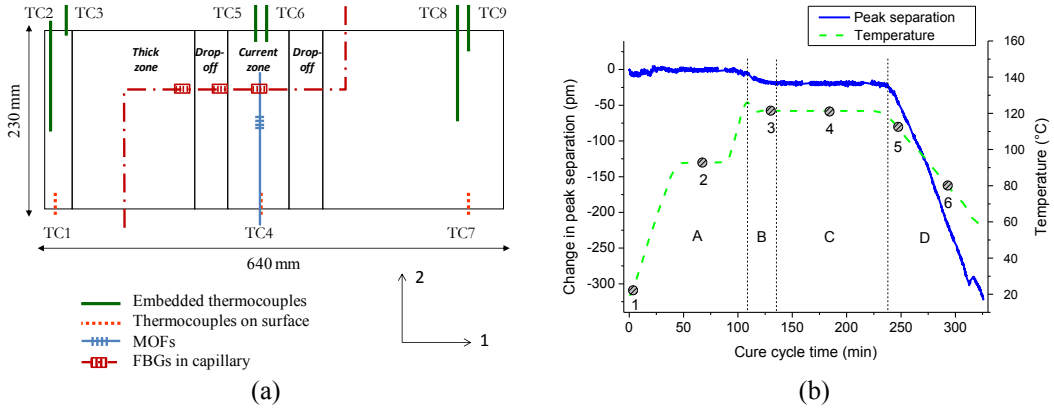

Figure 5: (a) Schematic of the optical fiber network embedded in the composite specimen. The coordinate system of the laminate is indicated. TC stands for thermocouple. (b) Changes in the temperature and in the peak separation Δλ during the entire cure cycle. The temperature profile is recorded with thermocouple TC6 (adapted from [27]).

4.2 Shear strain monitoring in glued lap joints

We have also shown that it is possible to measure shear strain in glued joints with a butterfly MOF that is embedded such that the transverse strain sensing axes of the MOF are aligned with the directions of principal stress in a shear loaded single lap adhesive joint (SLJ) [28]. The scheme of the embedded sensor and the measured change of the Bragg wavelength separation with applied load are shown in Figure 6. We obtained a shear stress sensitivity of about 60 pm/MPa, which corresponds to a shear strain sensitivity of 0.01 pm/µε. Compared to conventional birefringent fibers and as discussed in [28], our dedicated MOF design has a fourfold larger sensitivity. These

results also show that by changing the angular orientation of the butterfly MOF sensor it can be used for either shear strain sensing or for transverse strain sensing, which provides opportunities for multi-axial strain sensing with the same type of sensor [29].

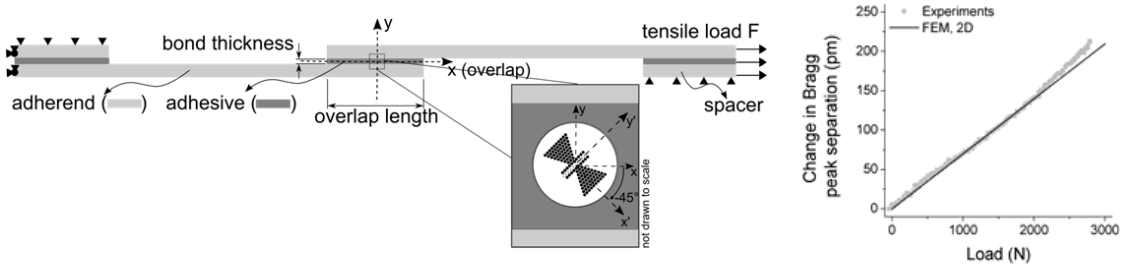

(a) (b)

Figure 6: (a) Configuration of the tested and modeled SLJ with an optical fiber embedded in the center of the adhesive layer. (b) The Bragg peak separation increases due to tensile loading with a sensor response of 67.4 pm/kN. Results from 2D FEM modeling of the SLJ are in very good agreement with the experimental results [28].

4.3 Temperature insensitive vibration monitoring

We have also built a polarimetric vibration sensor based on the Butterfly MOF [30]. A section of the MOF was subjected to a transversal force by means of a transducer that locally affects phase modal birefringence. This transducer is nothing else but a mechanical beam that transversally crushes the fiber over a 3 mm long section. The force is applied along one of the fiber's birefringence axes. When the transducer vibrates with a certain frequency, it induces a transversal force and hence a stress birefringence that also varies with that same frequency. To analyze the sensor response we used the so-called Stokes formalism (see also [30] for more details). The varying birefringence leads to a phase shift induced between the two polarization eigenmodes and results in a time varying state of polarization (SOP) at the output of the fiber. A polarization analyzer converts the varying SOP fluctuation into a varying optical output power. Depending on the vibration spectrum (frequency and acceleration amplitude), the stress induced birefringence varies as well as the optical output power. This allowed showing that the high sensitivity of the Butterfly MOF to transversal load leads to a more sensitive vibration sensor than 'Panda' type polarization maintaining fiber (PMF). The effect of temperature variations was also much less detrimental to the sensor response than when using Panda PMF. For an input sine-wave vibration, the peak-to-peak optical output variation of the sensor was only 10% over a temperature range from 25°C to 120°C.

CONCLUSION

We have introduced the principles of operation of a fiber Bragg grating based sensor inscribed in a highly birefringent microstructured optical fiber that has been designed so as to feature an enhanced sensitivity to transverse strain whilst being almost insensitive to temperature changes. We have illustrated how this sensor can be used in various applications that may support structural health monitoring, in particular three-dimensional strain measurements inside composite materials, cure process monitoring of and residual strain quantification in composite materials, shear stress monitoring in adhesive joints and temperature insensitive vibration monitoring.

ACKNOWLEDGEMENTS

The authors would like to acknowledge financial support from the Agency for Innovation by Science and Technology (IWT) for funding this research with the SBO Project grant 120024 'Self-Sensing Composites'. The authors also acknowledge the Research Foundation – Flanders (FWO), the Methusalem and Hercules Foundations Flanders, and the COST action TD1001.

REFERENCES

[1] O. Frazao, J.L. Santos, F. M. Araujo, L.A. Ferreira. Optical sensing with photonic crystal fibers. *Laser & Photonics Reviews*, 2(6):449-459, 2008.

[2] J. Canning. Properties of Specialist Fibres and Bragg Gratings for Optical Fiber Sensors. *Journal of Sensors*, 2012:598178, 2012.

[3] A.M.R. Pinto, M. Lopez-Amo, Photonic Crystal Fibers for Sensing Applications. *Journal of Sensors*, 2009:871580, 2009.

[4] O. Frazão, J. P. Carvalho, L. A. Ferreira, F. M. Araújo, J. L. Santos. Discrimination of strain and temperature using Bragg gratings in microstructured and standard optical fibres. *Measurement Science and Technology*, 16:2109-2113, 2005.

[5] H.R. Sørensen, J. Canning, J. Lægsgaard, K. Hansen. Control of the wavelength dependent thermooptic coefficients in structured fibres. *Optics Express*, 14(14):6428-6433, 2006.

[6] C. Chen, A. Laronche, G. Bouwmans, L. Bigot, Y. Quiquempois, J. Albert. Sensitivity of photonic crystal fiber modes to temperature, strain and external refractive index. *Optics Express*, 16(13):9645-9653, 2008.

[7] Y. Wang, H. Bartelt, W. Ecke, R. Willsch, J. Kobelke, M. Kautz, S. Brueckner, M. Rothhardt. Sensing properties of fiber Bragg gratings in small-core Ge-doped photonic crystal fibers. *Optics Communications*, 282:1129-1134, 2009.

[8] T. Geernaert, G. Luyckx, E. Voet, T. Nasilowski, K. Chah, M. Becker, H. Bartelt, W. Urbanczyk, J. Wojcik, W. De Waele, J. Degrieck, H. Terryn, F. Berghmans, H. Thienpont. Transversal Load Sensing With Fiber Bragg Gratings in Microstructured Optical Fibers. *IEEE Photonics Technology Letters*, 21(1):6-8, 2009.

[9] G. Luyckx, E. Voet, T. Geernaert, K. Chah, T. Nasilowski, W. De Waele, W. Van Paepegem, M. Becker, H. Bartelt, W. Urbanczyk, J. Wojcik, J. Degrieck, F. Berghmans, H. Thienpont. Response of FBGs in Microstructured and Bow Tie Fibers Embedded in Laminated Composite. *IEEE Photonics Technology Letters*, 21(18):1290-1292, 2009.

[10] J.-H. Zhang, N.-L. Liu, Y. Wang, L.-L. Ji, P.-X. Lu. Dual-Peak Bragg Gratings Inscribed in an All-Solid Photonic Bandgap Fiber for Sensing Applications. *Chinese Physics Letters*, 29(7):074205-1-4, 2012.

[11] L.A. Fernandes, M. Becker, O. Frazão, K. Schuster, J. Kobelke, M. Rothhardt, H. Bartelt, J.L. Santos, P.V.S. Marques. Temperature and Strain Sensing With Femtosecond Laser Written Bragg Gratings in Defect and Nondefect Suspended-Silica-Core Fibers, *IEEE Photonics Technology Letters*, 24(7):554-556, 2012.

[12] L. Jin, Z. Wang, Q. Fang, Y. Liu, B. Liu, G. Kai, X. Dong. Spectral characteristics and bend response of Bragg gratings inscribed in all-solid bandgap fibers. *Optics Express*, 15(23):15555-15565, 2007.

[13] L. Jin, W. Jin, J. Ju. Directional Bend Sensing With a CO_2-Laser-Inscribed Long Period Grating in a Photonic Crystal Fiber. *Journal of Lightwave Technology*, 27(21):4884-4891, 2009.

[14] T. Tenderenda, M. Murawski, M. Szymanski, L. Szostkiewicz, M. Becker, M. Rothhardt, H. Bartelt, P. Mergo, K. Poturaj, M. Makara, K. Skorupski, P. Marc, L.R. Jaroszewicz, T. Nasilowski. Longitudinal strain sensing with photonic crystal fibers and fiber Bragg gratings. *Proceedings of SPIE*, 8982:898219, March 2014.

[15] F. Berghmans, T. Geernaert, T. Baghdasaryan, H. Thienpont. Challenges in the fabrication of fibre Bragg gratings in silica and polymer microstructured optical fibres. *Laser & Photonics Reviews*, 8(1):27-52, 2014.

[16] T. Martynkien, G. Statkiewicz-Barabach, J. Olszewski, J. Wojcik, P. Mergo, T. Geernaert, C. Sonnenfeld, A. Anuszkiewicz, M. K. Szczurowski, K. Tarnowski, M. Makara, K. Skorupski, J. Klimek, K. Poturaj, W. Urbanczyk, T. Nasilowski, F. Berghmans, H. Thienpont. Highly birefringent microstructured fibers with enhanced sensitivity to hydrostatic pressure. *Optics Express*, 18(14):15113-15121, 2010.

[17] www.comsol.com

[18] F. Berghmans, T. Geernaert, M. Napierała, T. Baghdasaryan, C. Sonnenfeld, S. Sulejmani, T. Nasiłowski, P. Mergo, T. Martynkien, W. Urbanzcyk, E. Beres-Pawlik, H. Thienpont. Applying optical design methods to the development of application specific photonic crystal fibres. *Proceedings of SPIE*, 8550:85500B, 2012.

[19] S. Sulejmani, C. Sonnenfeld, T. Geernaert, P. Mergo, M. Makara, K. Poturaj, K. Skorupski, T. Martynkien, G. Statkiewicz-Barabach, J. Olzeswki, W. Urbanczyk, C. Caucheteur, K. Chah, P. Mégret, H. Terryn, J. Van Roosbroeck, F. Berghmans, H. Thienpont. Control Over the Pressure Sensitivity of Bragg Grating-Based Sensors in Highly Birefringent Microstructured Optical Fibers. *IEEE Photonics Technology Letters*, 24(6):527-529, 2012.

[20] C. Sonnenfeld, S. Sulejmani, T. Geernaert, S. Eve, N. Lammens, G. Luyckx, E. Voet, J. Degrieck W. Urbanczyk, P. Mergo, M. Becker, H. Bartelt, F. Berghmans, H. Thienpont. Microstructured Optical Fiber Sensors Embedded in a Laminate Composite for Smart Material Applications. *Sensors*, 11:2566-2579, 2011.

[21] G. Luyckx, E. Voet, W. D. Waele, J. Degrieck. Multi-axial strain transfer from laminated CFRP composites to embedded Bragg sensor: I. Parametric study. *Smart Materials and Structures,* 19(10): 105017, 2010.

[22] E. Voet, G. Luyckx, W. De Waele, J. Degrieck. Multi-axial strain transfer from laminated CFRP composites to embedded Bragg sensor: II. Experimental validation. *Smart Materials and Structures*, 19(10): 105018, 2010.

[23] C.M. Lawrence, D.V. Nelson, E. Udd, T. Bennett. A fiber optic sensor for transverse strain measurement. *Experimental Mechanics*, 39(3):202–209, 1999.

[24] D. V. Nelson, A. Makino, C. M. Lawrence, J. M. Seim, W. L. Schulz, E. Udd. Determination of the K-matrix for the multi-parameter fiber grating sensor in AD072 fibercore fiber. Proceedings of SPIE, 3489:79-85, September 1998..

[25] F. Berghmans, C. Sonnenfeld, S. Sulejmani, T. Geernaert, G. Luyckx, N. Lammens, J. Degrieck, E. Voet, K. Chah, F. Collombet, W. Urbanczyk, P. Mergo, M. Becker, H. Bartelt, H. Thienpont. Opportunities for Structural Health Monitoring of Composite Material Structures with novel Microstructured Optical Fiber Sensors. *Proceedings of 9th International Workshop on Structural Health Monitoring*, 1:902-909, September 2013.

[26] C. Sonnenfeld, G. Luyckx, F. Collombet, Y. Grunevald, B. Douchin, L. Crouzeix, M. Torres, T. Geernaert, S. Sulejmani, S. Eve, M. Gomina, K. Chah, P. Mergo, H. Thienpont, F. Berghmans. Embedded fibre Bragg gratings in photonic crystal fibres for cure cycle monitoring of carbon fibre reinforced polymer materials. *Proceedings of* SPIE, 8775:87750O, May 2013.

[27] C. Sonnenfeld, G. Luyckx, F. Collombet, Y-H. Grunevald, B. Douchin, L. Crouzeix, M. Torres, T. Geernaert, S. Sulejmani, K. Chah, P. Mergo, H. Thienpont, F. Berghmans. Cure cycle monitoring of laminated carbon fiber-reinforced plastic with fiber Bragg gratings in microstructured optical fiber. *Proceedings of the International Conference on Composite Materials 2013 (ICCM-19)*, 3327-3335, July-August 2013.

[28] S. Sulejmani, C. Sonnenfeld, T. Geernaert, G. Luyckx, D. Van Hemelrijck, P. Mergo, W. Urbanczyk, K. Chah, C. Caucheteur, P. Mégret, H. Thienpont, F. Berghmans. Shear stress sensing with Bragg grating-based sensors in microstructured optical fibers. *Optics Express*, 21(17):20404-20416 ,2013.

[29] S. Sulejmani, C. Sonnenfeld, T. Geernaert, D. Van Hemelrijck, G. Luyckx, P. Mergo, W. Urbanczyk, K. Chah, C. Caucheteur, P. Mégret, H. Thienpont, F. Berghmans, Fiber Bragg grating-based shear strain sensors for adhesive bond monitoring. *Proceedings of SPIE,* 9128:9128-12, April 2014.

[30] K. Chah, N. Linze, C. Caucheteur, P. Mégret, P. Tihon, O. Verlinden, S. Sulejmani, T. Geernaert, F. Berghmans, H. Thienpont, M. Wuilpart. Temperature-insensitive polarimetric vibration sensor based on HiBi microstructured optical fiber. *Applied Optics*, 51(25):6130-6138, 2012.